

RESEARCH ARTICLE

10.1002/2016JG003711

Key Points:

- Wavelet analysis and mechanistic modeling were applied to *Sphagnum* GPP calculated from NEE measured in situ at the Marcell Forest, Minnesota, USA
- Peak GPP was delayed relative to peak photosynthetically active radiation
- An interaction of the water table with *Sphagnum* photosynthesizing tissue area was the likely cause of delayed peak GPP

Supporting Information:

- Supporting Information S1

Correspondence to:

A. P. Walker,
walkerap@ornl.gov

Citation:

Walker, A. P., K. R. Carter, L. Gu, P. J. Hanson, A. Malhotra, R. J. Norby, S. D. Sebestyen, S. D. Wullschlegler, and D. J. Weston (2017), Biophysical drivers of seasonal variability in *Sphagnum* gross primary production in a northern temperate bog, *J. Geophys. Res. Biogeosci.*, 122, 1078–1097, doi:10.1002/2016JG003711.

Received 16 NOV 2016

Accepted 7 APR 2017

Accepted article online 18 APR 2017

Published online 6 MAY 2017

©2017. American Geophysical Union.
All Rights Reserved.

This manuscript has been authored by UT-Battelle, LLC under contract DE-AC05-00OR22725 with the U.S. Department of Energy. The United States Government retains and the publisher, by accepting the article for publication, acknowledges that the United States Government retains a nonexclusive, paid-up, irrevocable, worldwide license to publish or reproduce the published form of this manuscript, or allow others to do so, for United States Government purposes. The Department of Energy will provide public access to these results of federally sponsored research in accordance with the DOE Public Access Plan (<http://energy.gov/downloads/doe-public-access-plan>).

Biophysical drivers of seasonal variability in *Sphagnum* gross primary production in a northern temperate bog

Anthony P. Walker¹ , Kelsey R. Carter², Lianhong Gu¹ , Paul J. Hanson¹ , Avni Malhotra¹ , Richard J. Norby¹, Stephen D. Sebestyen³ , Stan D. Wullschlegler¹ , and David J. Weston²

¹Climate Change Science Institute and Environmental Sciences Division, Oak Ridge National Laboratory, Oak Ridge, Tennessee, USA, ²Climate Change Science Institute and Biosciences Division, Oak Ridge National Laboratory, Oak Ridge, Tennessee, USA, ³Northern Research Station, USDA Forest Service, Grand Rapids, Minnesota, USA

Abstract *Sphagnum* mosses are the keystone species of peatland ecosystems. With rapid rates of climate change occurring in high latitudes, vast reservoirs of carbon accumulated over millennia in peatland ecosystems are potentially vulnerable to rising temperature and changing precipitation. We investigate the seasonal drivers of *Sphagnum* gross primary production (GPP)—the entry point of carbon into wetland ecosystems. Continuous flux measurements and flux partitioning show a seasonal cycle of *Sphagnum* GPP that peaked in the late summer, well after the peak in photosynthetically active radiation. Wavelet analysis showed that water table height was the key driver of weekly variation in *Sphagnum* GPP in the early summer and that temperature was the primary driver of GPP in the late summer and autumn. Flux partitioning and a process-based model of *Sphagnum* photosynthesis demonstrated the likelihood of seasonally dynamic maximum rates of photosynthesis and a logistic relationship between the water table and photosynthesizing tissue area when the water table was at the *Sphagnum* surface. The model also suggested that variability in internal resistance to CO₂ transport, a function of *Sphagnum* water content, had minimal effect on GPP. To accurately model *Sphagnum* GPP, we recommend the following: (1) understanding seasonal photosynthetic trait variation and its triggers in *Sphagnum*; (2) characterizing the interaction of *Sphagnum* photosynthesizing tissue area with water table height; (3) modeling *Sphagnum* as a “soil” layer for consistent simulation of water dynamics; and (4) measurement of *Sphagnum* “canopy” properties: extinction coefficient (k), clumping (Ω), and maximum stem area index (SAI).

1. Introduction

Northern peatlands are estimated to store 547 (473–621) Pg of carbon (C) [Yu *et al.*, 2010], as much as one fifth to one third of Earth’s nonpermafrost soil C [Ciais *et al.*, 2014]. Peat is formed by extremely slow decomposition and compression of plant material, primarily biomass from *Sphagnum* peat mosses [Clymo, 1970, 1984]. Peat accumulates when long-term primary production exceeds the sum of C respired during decomposition and dissolved C export [Clymo, 1984; Roulet *et al.*, 2007]. Climatic conditions, in part, have caused northern peatlands to be C sinks since the last glaciation [Armentano and Menges, 1986; Billings, 1987; Gorham, 1991; Yu *et al.*, 2010; Gorham *et al.*, 2012]. However, the rapidly changing climate in the high latitudes is likely to change both primary production and decomposition rates, with the potential to reverse the millennial timescale peatland carbon sink over potentially much shorter timescales [Moore *et al.*, 1998; Turetsky *et al.*, 2002; Wu and Roulet, 2014]. A greater understanding of peatland C cycling (i.e., production and decomposition) across space and through time is thus a research priority [Limpens *et al.*, 2008; Strack *et al.*, 2008] that needs to be pursued to advance current wetland modeling efforts [Wania *et al.*, 2009; Shi *et al.*, 2015].

In this study we focus on *Sphagnum* gross primary production (GPP), a key component of northern peatland C cycling. *Sphagnum* is considered a dominant genus in northern peatlands, often present as a continuous understory layer and forming an estimated 50% of accumulated peat [Rydin *et al.*, 2013]. *Sphagnum* is also an ecosystem engineer, maintaining low pH and decomposition rates in its surrounding environment, thus promoting peat accumulation and further *Sphagnum* production [van Breemen, 1995]. *Sphagnum* net primary production (NPP) is highly variable globally and related to water table, temperature [Gunnarsson, 2005], and growing season integrated photosynthetically active radiation [Loisel *et al.*, 2012]. To simulate NPP, most peatland modeling efforts rely on empirical models (usually as a function of water table) rather than process-based, mechanistic models [Belyea and Malmer, 2004; Wania *et al.*, 2009; Froliking *et al.*, 2010;

Kleinen et al., 2012]. Few modeling efforts are based on mechanistic models of *Sphagnum* ecophysiology or peat production [but see St-Hilaire et al. [2010] and Dimitrov et al. [2011]].

In part due to different timescales of application, empirical methods for modeling peatlands contrast with the majority of C cycle/land surface models (referred to hereafter as terrestrial ecosystem models TEMs) used to predict the response of the C cycle to increasing CO₂ and climate change over the coming century. TEMs commonly employ mechanistic representations of photosynthesis and other biogeochemical and biogeophysical processes to simulate GPP and NPP [Pitman, 2003; Fisher et al., 2014]. A first step in aligning *Sphagnum* production models with the core assumptions of these TEMs will be a mechanistic understanding of *Sphagnum* GPP and its drivers, allowing TEMs to predict gross peatland C uptake under possible future precipitation and temperature regimes in a way that is consistent with their simulation of other plant functional types [Frolking et al., 2009].

In contrast to vascular plants, *Sphagnum* are poikilohydric and cannot actively regulate water loss because they lack the following: stomata, a waxy cuticle, and well-defined water conduction vessels [Frolking et al., 2009; Weston et al., 2015]. Thus, for *Sphagnum*, and other poikilohydric genera, the water status of the environment is likely an even more important determinant of photosynthesis and growth than for vascular plants [Dimitrov et al., 2011]. Unlike other poikilohydric genera, *Sphagnum* possess hyaline cells which are dead cells that encase the living cells of the *Sphagnum* providing water retention, much like a sponge, as well as a habitat for associated microbiota [Weston et al., 2015; Kostka et al., 2016]. Nevertheless, *Sphagnum* tissue water content can only be maintained passively by inputs from precipitation, external capillary movement, and water storage in the hyaline cells [Schipperges and Rydin, 1998]. *Sphagnum* photosynthetic capacity and resistance to CO₂ diffusion to the site of carboxylation are dependent upon tissue water content [Williams and Flanagan, 1996, 1998; Hanson et al., 2014]. Thus, seasonal variation in water availability is likely to contribute strongly to the seasonality of photosynthetic C fluxes [Backéus, 1988; Adkinson and Humphreys, 2011; Dimitrov et al., 2011].

Along with water, temperature is also a likely factor that contributes to seasonal variability in *Sphagnum* C fluxes. In the northern latitudes where climatic conditions are favorable for bog ecosystems to establish, the length of the growing season is determined by spring thaw and autumn freeze. Physiologically, and similar to many vascular plants, temperature has a positive correlation with *Sphagnum* photosynthesis until an optimum is reached, followed by a decline [Hanson et al., 1999; Maseyk et al., 1999]. Also, Williams and Flanagan [1998] demonstrated seasonal variability in *Sphagnum* photosynthetic capacity, perhaps linked to temperature, while dark respiration was relatively constant throughout the growing season.

While GPP cannot be directly measured in the field, a common and useful practice is to partition net ecosystem exchange (NEE; measured using eddy covariance techniques or closed path chambers) into its component fluxes GPP and ecosystem respiration (R_e) using empirical regressions [Barr et al., 2004; Reichstein et al., 2005]. Many studies in the literature use eddy covariance and flux partitioning in ecosystems dominated by vascular plants, while fewer studies exist in ecosystems dominated by nonvascular plants. Numerous measurements of peatland NEE in situ have been made using eddy-covariance techniques [Humphreys et al., 2006; Syed et al., 2006; Adkinson et al., 2011; Dise et al., 2011; Sulman et al., 2012; Olson et al., 2013]. However, these eddy-covariance measurements include fluxes from both the vascular and nonvascular plant components of the ecosystem. Fewer studies exist where only the *Sphagnum* NEE is captured, typically using chamber measurements [Wieder et al., 2009; Cai et al., 2010; Adkinson and Humphreys, 2011]. A comprehensive understanding of interacting and seasonally variable influences of temperature and water on *Sphagnum* GPP in the field is lacking and necessary to incorporate *Sphagnum* as a plant functional type into TEMs.

Here we combine empirical data with statistical and mechanistic modeling to improve the mechanistic understanding of the biophysical drivers of *Sphagnum* GPP. The aim of this study is to characterize the effects of water, temperature, and light on the seasonal dynamics of *Sphagnum* GPP. At the S1 bog of the Marcell Experimental Forest, in situ *Sphagnum*-peat hourly NEE was measured using a LICOR 8100 system and GPP was estimated using empirical flux [Barr et al., 2004]. Wavelet coherence analysis is used to identify relationships among GPP and its biophysical drivers in the frequency and time domains within the growing season. Lastly, a simple, mechanistic *Sphagnum* photosynthesis model [Williams and Flanagan, 1998; Weston et al., 2015] is used to help investigate and assess quantitative understanding of the drivers of *Sphagnum* GPP. We use the model as a set of mathematically defined hypotheses to illuminate which hypotheses are

necessary to explain the dominant modes of variability in *Sphagnum* GPP estimated by net gas exchange and flux partitioning. The specific hypotheses, as defined below in the methods, describe the light response of photosynthesis according to *Farquhar et al.* [1980], *Harley et al.* [1992], and *Sellers et al.* [1992], with the light extinction coefficient modified for *Sphagnum* after *Williams and Flanagan* [1998]. Also investigated is the influence of the *Sphagnum* “canopy” clumping [*Niinemets and Tobias*, 2014] and stem area index (SAI). The temperature response is hypothesized as a modified Arrhenius relationship [*Medlyn et al.*, 2002]. Hypotheses on the effect of water table are based on internal resistance to CO₂ diffusion as a function of *Sphagnum* water content [*Williams and Flanagan*, 1998] and a boundary layer resistance caused by water when the *Sphagnum* are submerged.

2. Materials and Methods

2.1. Experimental Site

This study is located at the site of the Spruce and Peatland Responses Under Climatic and Environmental Change—SPRUCE—experiment [<http://mnspruce.ornl.gov>; *Hanson et al.*, 2017; *Krassovski et al.*, 2015] on the S1 bog of the Marcell Experimental Forest [47.506°N, 93.453°W, 418 m above mean sea level; *Sebestyen et al.*, 2011]. The S1 bog is a weakly ombrotrophic peatland with a perched water table that has limited groundwater influence [*Griffiths and Sebestyen*, 2016]. The S1 bog has a hummock-hollow microtopography with a nearly complete cover of *Sphagnum* mosses. *Sphagnum magellanicum* (Brid.) comprises approximately 20% of the moss layer, primarily in the hummocks, *Sphagnum fallax* Klinggr. comprises 15%, primarily in the hollows, and *Sphagnum angustifolium* (C.E.O. Jensen ex Russow) C.E.O. Jensen comprises 55% with a presence in both hummocks and hollows. However, we note that separating *S. fallax* and *S. angustifolium* in the field is quite difficult. In addition, non-*Sphagnum* mosses (*Polytrichum* spp., 4% cover and feather mosses, 3% cover) are present on hummocks. *Picea mariana* (Mill.) and *Larix laricina* (Du Roi) overtop the bog with woody shrubs and forbs in the understorey. The trees of the S1 bog were harvested in strip cuts in 1969 and 1974. In its current state of regrowth the canopy is 5–8 m tall. The peatland soil is the Greenwood series a Typic Haplohemist (<http://websoilsurvey.nrcs.usda.gov>) with average peat depths to the Wisconsin glacial-age lake bed of 2 m to 3 m [*Parsekian et al.*, 2012].

The climate of the Marcell Experimental Forest is subhumid continental, with wide and rapid diurnal and seasonal temperature fluctuations [*Sebestyen et al.*, 2011]. Over the period from 1961 to 2005, the average annual air temperature was 3.3°C, with extremes in the daily mean of –38°C and 30°C, and the average annual precipitation was 768 mm. Mean annual air temperatures have increased about 0.4°C per decade over the last 40 years [*Sebestyen et al.*, 2011]. At SPRUCE a vertical profile of air and soil temperature measurements are recorded, and photosynthetically active radiation (PAR) sensors are installed in multiple locations [*Hanson et al.*, 2011; *Hanson et al.*, 2015]. Water table measurements were measured as part of the long-term research program of the Forest Service at the Marcell Experimental Forest [*Sebestyen et al.*, 2011]. Water tables have been recorded by a float-driven stripchart recorder and reported as daily maximum water table elevations since measurements began during 1960.

2.2. NEE Field Measurements

In June 2014, six automated 8100-104C 20 cm diameter clear top chambers (LI-COR, Lincoln, Nebraska, USA) and the associated control system (LI-8100A; LI-COR, Lincoln, Nebraska, USA) were installed in the S1 bog (Figure 1) to measure *Sphagnum*-peat CO₂ uptake from the atmosphere. Hereafter we refer to *Sphagnum*-peat CO₂ uptake as NEE while recognizing this is not true NEE as there are fluxes from other components of the ecosystem that we have not quantified. Three chambers per dominant species (*S. magellanicum* or *S. fallax*) were placed in the bog in relatively open ground where there was little clear hummock-hollow definition (Figure 1). The automated chambers are designed to minimize PAR attenuation, equalize chamber pressure with the atmosphere, and maintain a well-mixed air sample. They were programmed to take a 120 s air sample from each chamber every hour and use a dead band of 30 s. Measurements were made on 6 June to 6 November 2014 and 20 March to 10 May 2015 on which date the instrument failed—a hazard of working with such water-sensitive instruments in a water-saturated environment. Water table height is expressed with zero at the *Sphagnum* surface, which was estimated from observations of when the *Sphagnum* in the chambers were submerged, although there was some variability (± 20 mm) in the mean *Sphagnum* surface height. A positive water table height represents the water table above the *Sphagnum*.



Figure 1. Field placement of the LICOR 8100 clear top soil respiration chambers in the *Sphagnum* at the SPRUCE experiment, Marcell Experimental Forest, Minnesota.

semishaded measurements in hollows as the 8100 chambers were sited in a relatively open position (Figure 1).

In brief, the flux-partitioning method derived empirical flux-environment relationships for R_e and GPP. For R_e an empirically derived Q_{10} relationship of nighttime C fluxes (i.e., R_e) with temperature (T) and water table height (W_h) was used to calculate all daytime R_e data and missing nighttime R_e (<2% of nighttime data) from measured T and W_h . GPP was calculated by summing R_e and NEE. An empirical relationship of GPP with PAR and W_h was then calculated and used to gap fill missing GPP values (<2% of the time series). Finally, NEE was gap filled (<2% of time series) by subtracting the calculated R_e from GPP.

Following the method of Barr *et al.* [2004], for both R_e and GPP, a second time-varying empirical correction was calculated to account for temporal variance, i.e., systematic errors, in the flux-environment relationship. The time-varying scalar was used to empirically correct the flux-environment relationships during periods of gap filling (daytime R_e and GPP during periods of missing NEE data). The scalar was calculated as the slope of a linear regression (forced through the intercept) between fluxes, nighttime R_e or GPP calculated from NEE and flux-partitioned R_e , and fluxes calculated using the flux-environment relationship [Barr *et al.*, 2004], equations (1) and (2), respectively. The time-varying parameter was calculated for each nonmissing datum using the 100 data points surrounding the datum in question [Barr *et al.*, 2004]; the time span that the window encompassed was therefore variable due to missing data. Once calculated for all time points with nonmissing data, the time-varying parameter was interpolated to time points with missing data using the linear interpolation function “na.approx” in R [R Core Development Team, 2016]. Results suggest that systematic errors in the calculation of R_e were small (see section 3 below), albeit that this method cannot account for systematic differences in the empirical relationships of daytime and nighttime R_e to environment.

2.3. Partitioning NEE into GPP and R_e

Data processing and analysis were done in R [R Core Development Team, 2016]. Hourly *Sphagnum*-peat NEE flux data from the 8100 chambers were partitioned into the component fluxes R_e and GPP using empirical relationships to temperature and light based on the method of Reichstein *et al.* [2005] and Barr *et al.* [2004], modified to account for the influence of water table height on C fluxes in this water-sensitive *Sphagnum*-peat system. Including water table height in the empirical relationships resulted in models with lower Akaike Information Criterion (AIC). At SPRUCE a vertical profile of air and soil temperature measurements are recorded, and for the flux partitioning, we used the temperature at 100 mm above the mean hummock height as this explained the most variation in nighttime R_e —see D’Angelo *et al.* [2016] for an investigation of synchronizing temperatures and flux measurements. PAR used was a mean of open-sky measurements situated above the bog surface and

The exact form of the empirical function for calculating daytime and gap-filling missing nighttime values of R_e was as follows:

$$R_e = r(t)(r_b + r_w W_h) Q_{10}^{\frac{T-10}{10}}, \quad (1)$$

where $r(t)$ is the time-varying scalar (unitless), r_b is the base respiration rate at 10°C ($\mu\text{mol m}^{-2} \text{s}^{-1}$), r_w scales the effect of water table height on the base respiration rate ($\mu\text{mol m}^{-2} \text{s}^{-1} \text{mm}^{-1}$), and Q_{10} is the factor by which respiration rate increases for each 10°C increase in T . In addition to the Q_{10} relationship with temperature, we tested a logistic function [following Barr *et al.*, 2004] and an Arrhenius function. All three functional forms had very similar AIC values (<1% difference).

The exact form of the empirical function to gap fill GPP was as follows:

$$\text{GPP} = g(t) \left[\frac{\alpha \text{PAR}(g_{\max} + g_w W_h)}{\alpha \text{PAR} + (g_{\max} + g_w W_h)} \right], \quad (2)$$

where $g(t)$ is the time-varying scalar (unitless), g_w scales the effect of water table height on g_{\max} ($\mu\text{mol m}^{-2} \text{s}^{-1} \text{mm}^{-1}$), α is the light use efficiency (mol C mol e^{-1}), and g_{\max} is the maximum GPP at light saturation ($\mu\text{mol m}^{-2} \text{s}^{-1}$). The functions were fit with nonlinear least squares using the “nls” function in R [R Core Development Team, 2016]. The flux partitioning algorithm was applied separately to the data from each individual 8100 chamber. Empirical functions for R_e and GPP were also developed that did not include water table height as an explanatory variable; these provided a worse fit to the data but did not qualitatively change the flux partitioning.

2.4. Wavelet Analysis

Wavelet analysis allows investigation of the relationships of periodic phenomena between time series in the period/frequency and time domains [Roesch and Schmidbauer, 2014] and has been previously applied to eddy covariance time series in vascular plant ecosystems [Stoy *et al.*, 2009] and simulation model performance in similar ecosystems [Dietze *et al.*, 2011]. We used wavelet analysis to test the correlation between GPP and temperature, PAR, and water table depth at timescales ranging from days to months. Wavelet analysis was conducted in R with the package “waveletComp” [Roesch and Schmidbauer, 2014].

2.5. Modeling *Sphagnum* Photosynthesis

A simple “canopy”-scale *Sphagnum* photosynthesis model was used to investigate the drivers of GPP. The multiassumption architecture and test bed (MAAT v0.5.1; <https://github.com/walkeranthony/MAAT>), written in R, was used as a framework for the *Sphagnum* model. The *Sphagnum* photosynthesis model is based on that of Williams and Flanagan [1998] and is similar to that used in Weston *et al.* [2015]. The model was made specific to *Sphagnum* by accounting for tissue resistance to CO_2 transport from the atmosphere to the chloroplast, after Williams and Flanagan [1998], and when the *Sphagnum* were submerged, the resistance of the water layer was calculated based solely on diffusion. High extinction coefficients for light penetration into the *Sphagnum* “canopy” were used [Williams and Flanagan, 1998].

The model is based on the enzyme kinetic model of photosynthesis by Farquhar *et al.* [1980]. Net CO_2 assimilation (A , $\mu\text{mol C m}^{-2} \text{s}^{-1}$) is the minimum of the RuBisCO limited carboxylation rate (w_c , $\mu\text{mol C m}^{-2} \text{s}^{-1}$) and the electron transport limited carboxylation rate (w_j , $\mu\text{mol C m}^{-2} \text{s}^{-1}$), scaled to account for photorepiration, minus mitochondrial respiration (R_d). The net assimilation function takes the following form:

$$A = \min\{w_c, w_j\} (1 - \Gamma^*/C_c) - R_d, \quad (M1)$$

where Γ^* is the CO_2 compensation point (Pa) in the absence of mitochondrial respiration; i.e. the C_c (CO_2 concentration at the site of carboxylation; Pa) at which the carboxylation rate is balanced by CO_2 release from oxygenation. R_d was assumed to be 10% of V_{cmax} [Williams and Flanagan, 1998]. Both w_c and w_j are modeled as functions of C_c . w_c follows a Michaelis-Menten function of C_c in which V_{cmax} (the maximum carboxylation rate of RuBisCO; $\mu\text{mol C m}^{-2} \text{s}^{-1}$) determines the asymptote:

$$w_c = V_{\text{cmax}} \frac{C_c}{C_c + K_c (1 + O_i/K_o)}, \quad (M2)$$

where O_i is the intercellular O_2 partial pressure (kPa); K_c (Pa) and K_o (kPa) are the Michaelis-Menten constants of RuBisCO for CO_2 and for O_2 . K_c and K_o were parameterized after Bernacchi *et al.* [2003] and Γ^* after

Table 1. Parameter Values Used in the *Sphagnum* Photosynthesis Model, Taken From *Williams and Flanagan* [1998] and *Medlyn et al.* [2002]^a

Parameter	Units	Value
V_{cmax}	$\mu\text{mol C m}^{-2} \text{s}^{-1}$	14.4
J_{max}	$\mu\text{mol e m}^{-2} \text{s}^{-1}$	25.6
a	—	0.8
α_i	$\mu\text{mol e } \mu\text{mol}^{-1} \text{ photons}$	0.3125
H_a	J mol^{-1}	69,830
H_d	J mol^{-1}	200,000
$T_{opt} (V_{cmax})$	$^{\circ}\text{C}$	27.56
$T_{opt} (J_{max})$	$^{\circ}\text{C}$	19.89
SAI	$\text{m}^2 \text{m}^{-2}$	2 (1, 3, 4)
k	—	1.5 (1)
Ω	—	1 (0.5)
p_1 (maxSAI)	$\text{m}^2 \text{m}^{-2}$	na (3)
p_2	—	na (0.2)
p_3	$\ln(\text{mm}^{-1})$	na (0.1, 0.3, 0.5, 1)

^aValues in parentheses indicate nondefault values that were used in the ensemble of simulations. na indicates that the function that uses these parameters were not used in the main ensemble, i.e., they were only employed for the simulations shown in Figure 9.

Brooks and Farquhar [1985]. The light limited carboxylation rate (w_j) is a function of the electron transport rate (J , $\mu\text{mol e m}^{-2} \text{s}^{-1}$) following a similar function of C_c where the asymptote is proportional to J :

$$w_j = \frac{J}{4} \frac{C_c}{(C_c + 2\Gamma_*)} \quad (\text{M3})$$

J is a function of incident photosynthetically active radiation (PAR — $\mu\text{mol photons m}^{-2} \text{s}^{-1}$) that saturates at the maximum rate of electron transport (J_{max} , $\mu\text{mol e m}^{-2} \text{s}^{-1}$), formulated by *Harley et al.* [1992] following *Smith* [1937], although other formulations exist:

$$J = \frac{a\alpha_i \text{PAR}}{\left[1 + \left(\frac{a\alpha_i \text{PAR}}{J_{max}}\right)^2\right]^{0.5}} \quad (\text{M4})$$

where a is the fraction of light absorbed by the leaf (assumed 0.8), α is the intrinsic quantum efficiency of electron transport (we used $0.3215 \text{ mol electrons mol}^{-1} \text{ photons}$ to be consistent with an apparent quantum efficiency of 0.25 after *Williams and Flanagan* [1998]). The exponents in equation (M4) are empirical values and represent the transition from light-limiting to maximum rate-limiting conditions.

C_c is determined by Fick's law:

$$C_c = C_a - r_i A p, \quad (\text{M5})$$

where C_a is the atmospheric CO_2 partial pressure (Pa), p is atmospheric pressure (MPa), and r_i is the internal resistance to CO_2 ($\text{m}^2 \text{s mol}^{-1} \text{ C}$). Water resistance to CO_2 transfer when the *Sphagnum* were submerged was assumed to occur only via diffusion and was simulated analogously to a leaf boundary layer resistance using the diffusion equation presented in *Evans et al.* [2009] to calculate the resistance term.

To test the influence of *Sphagnum* water content on C assimilation, we employed a number of assumptions to simulate r_i : (1) zero r_i (i.e., $C_c = C_a$); (2) r_i is constant based on the mean of: (3) r_i is a function of fresh mass to dry mass ratio (W) [*Williams and Flanagan*, 1998]:

$$g_i = 10^3 (-0.195 + 0.134W - 0.0256W^2 - 0.000984W^4 + 0.0000168W^5). \quad (\text{M6})$$

where g_i is the internal conductance to CO_2 diffusion and is the inverse of r_i . *Sphagnum* dry mass to fresh mass ratio (W) was simulated as a simple linear function of water table height after *Adkinson and Humphreys* [2011].

Temperature scaling was achieved by the modified Arrhenius equation described by *Medlyn et al.* [2002]:

$$S_{T,T_r} = \exp\left(\frac{H_a(T - T_r)}{RTT_r}\right) \frac{1 + \exp\left(\frac{\Delta S T_r - H_d}{RT_r}\right)}{1 + \exp\left(\frac{\Delta S T - H_d}{RT}\right)}, \quad (\text{M7})$$

where S_{T,T_r} is the scalar to scale a value from a reference temperature T_r to an environment temperature T , exp is the exponential function, H_a and H_d are the activation and deactivation energy, R is the universal gas constant, and

$$\Delta S = \frac{H_d}{T_{opt}} + R \log\left(\frac{H_a}{(H_d - H_a)}\right), \quad (\text{M8})$$

where T_{opt} is the optimum temperature. Temperature sensitivity for V_{cmax} and J_{max} was based on parameters for *Pinus sylvestris* [*Medlyn et al.*, 2002] which, although very clearly a different plant functional type, occupy similar climatic environments and share a similar temperature optimum around 25°C [*Harley et al.*, 1989].

Simulation of the *Sphagnum* “canopy” was achieved by simulating a multilayer canopy (i.e., photosynthesis calculations were made in each layer) with the number of layers determined by the SAI. Incident light was assumed as direct beam, and light scaling was implemented using Beer’s Law [Monsi and Saeki, 1953; Sellers et al., 1992; Wang, 2003], which assumes homogenous distribution of the leaves in the plane perpendicular to the incident light. We accounted for the highly aggregated distribution of *Sphagnum* in that plane by including a clumping coefficient, Ω [Niinemets and Tobias, 2014]:

$$I_i = I_0 e^{-\Omega k(S)} \quad (\text{M9})$$

where I_i is the light incident in layer i , I_0 is the incident light at the top of the canopy (i.e., measured PAR), k is the canopy light extinction coefficient, and S is the canopy layer, i.e., the cumulative shoot area index. Following Williams and Flanagan [1998], we employed a k of 1.5 for *Sphagnum* though recognizing that this is above the bounds of physical possibility for this parameter (0–1) which describes the 2D projected area of a single layer shoot/leaf as a fraction of the 2D plane perpendicular to the light direction. Unlike Williams and Flanagan [1998], we use (S) and not $(S - 1)$ in the exponent of equation (M9), (S) is the correct form for the solution of the two-stream approximation when scattering is ignored [Wang, 2003; see also Sellers et al., 1992; and Niinemets and Tobias, 2014]. As a simplifying assumption, we did not account for diffuse radiation nor variation in the solar zenith angle. We assumed V_{cmax} and J_{max} were the same in each shoot layer.

A logistic function was also tested to describe the relationship between SAI and water table, when the water table was close to the *Sphagnum* surface height. The need for this hypothesis is described below in the results and discussion. The function is as follows:

$$\text{SAI} = \frac{p_1 p_2}{p_2 + e^{-p_3 W_t}}, \quad (\text{M10})$$

where p_1 is the maximum SAI, p_2 primarily controls the value of W_t when SAI is $p_1/2$ (when $p_2 = 1$, $W_t = 0$ when $\text{SAI} = p_1/2$), and p_3 controls the gradient of the curve and also the W_t range between zero and maximum SAI.

The “canopy”-scale *Sphagnum* photosynthesis model was run at each half-hourly time point in the meteorological data set over the measured time period from 7 June to 7 November 2014 and 27 March to 4 May 2015. Instantaneous fluxes were assumed to represent the whole half-hour period and were scaled by the number of seconds in a half hour. Parameters used in the model are shown in Table 1. The model was run with a number of CO_2 transport resistance assumptions to tease out various influences of water on GPP. *Sphagnum* resistance (r_i) to CO_2 transport was assumed to be either zero, variable according to the function of fresh weight dry weight ratio of Williams and Flanagan [1998], or constant at the mean value from variable resistance simulation. In an informal sensitivity analysis, the model was run with combinations of SAI (1–4), k (1 and 1.5), Ω (0.5 and 1), and p_3 (0.1, 0.3, 0.5, 1.0) to investigate the GPP prediction space from the various modeling hypotheses.

3. Results

3.1. Site Meteorology

Primary meteorological variables integrated daily PAR and mean diel temperature (10 cm above hummock height, see Figure S1 in the supporting information for temperature at different heights or at the hourly time-scale) showed a typical southern boreal seasonal cycle (Figure 2a). Peak temperatures were shifted later in the year compared to peak PAR and showed a broader peak that lasted from early July, through August and into early September (Figure 2a). Water table height relative to *Sphagnum* surface in the chambers was negative through the frozen winter and early spring. During thaw and rainfall in spring, water table showed a large increase to peak levels, submerging the *Sphagnum*, which then declined through summer to reach a minimum at the end of the broad temperature peak (Figure 2b).

Due to logistics and equipment failure when water tables were high, it was necessary to combine 2 years of data (2014 and 2015) to investigate the growing season cycle. The LI-8100 was operational in the early summer through the autumn of 2014 (6 June to 6 November) and the early spring of 2015 (20 March to 10 May); see the highlighted regions in Figure 2. In all further time series figures, we present the 2015 data first to illustrate a near complete growing season cycle. The composite seasonal cycle, formed by these two seasons, captured much of the key features of the full seasonal cycles described above (Figure 3). Peak values of PAR and temperature were $46 \text{ mol m}^{-2} \text{ d}^{-1}$ and 20°C . The early frozen period of the growing season was

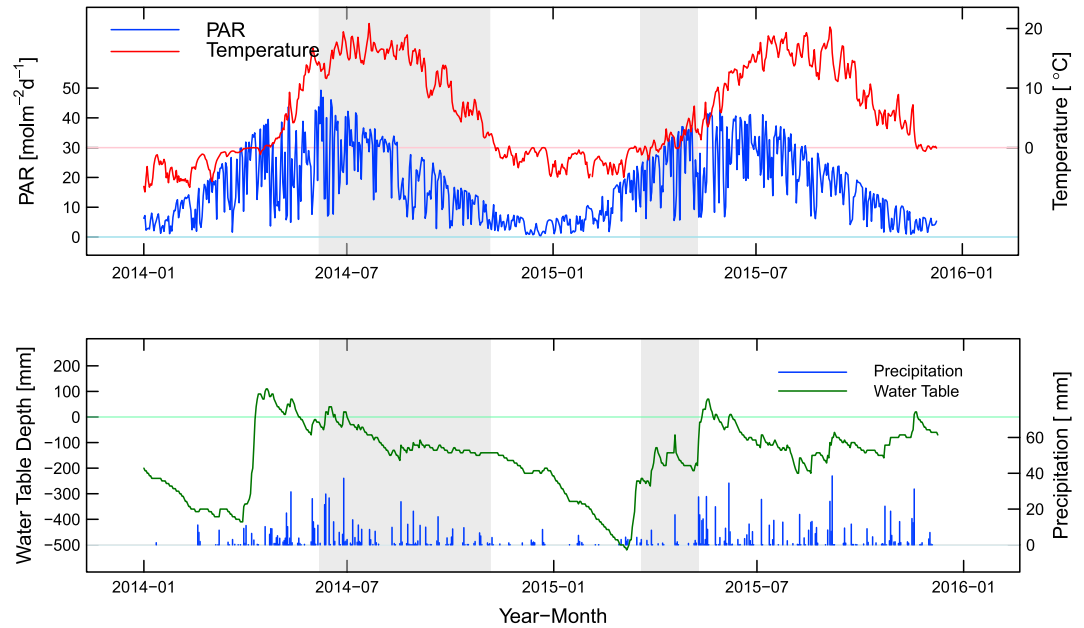


Figure 2. Site environmental data for full years 2014 and 2015. (a) Daily integrated values for photosynthetically active radiation (PAR, $\mu\text{mol m}^{-2} \text{s}^{-1}$) and diel mean temperature at 10 cm above the hummock surface ($^{\circ}\text{C}$) and (b) precipitation and water table depth (both mm). Shaded areas represent the periods for which we have measurements from the 8100 s.

captured in the 2015 data. Peak PAR, the broad temperature peak, and brief submergence of the *Sphagnum* followed by a decline in water table were all captured in the 2014 data. Spring snowmelt and midsummer precipitation events led to water table peaks of around 45 mm and 20 mm and gradually declined to a mean value of -105 ± 20 mm from early-August to November of 2014 (Figure 3). Declining PAR and temperature approaching zero were captured in the autumn of 2014. Unfortunately, the thaw in spring of 2015 was the cause of the instrument failure, and therefore, we missed this important period of the seasonal cycle.

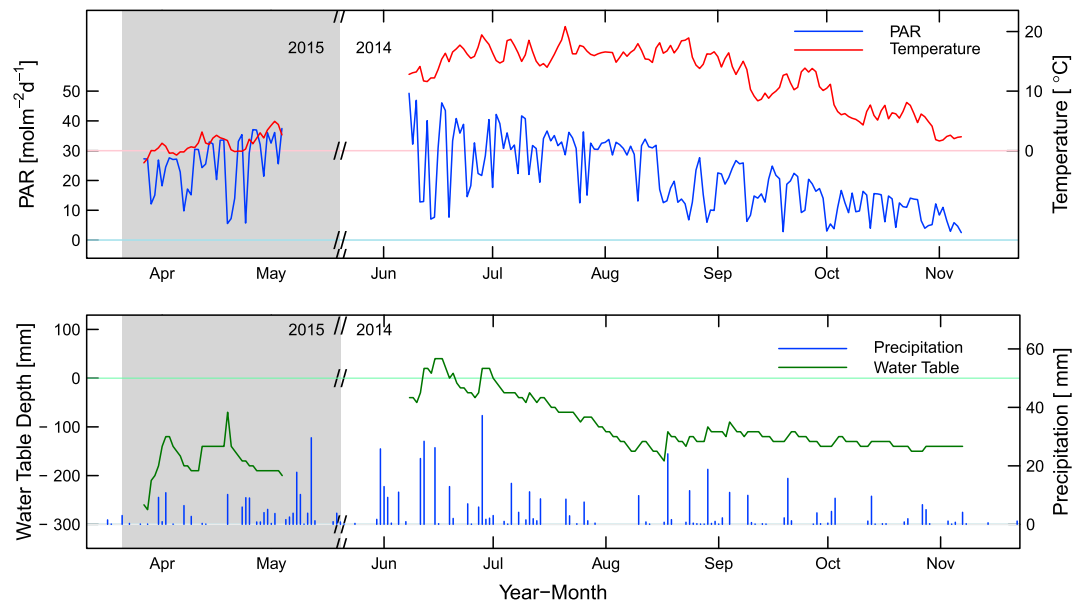


Figure 3. Site environmental data for the composite growing season; see Figure 2 legend for more details. The 2015 data presented before 2014 to illustrate the seasonal cycle. Shaded area represents 2015 data.

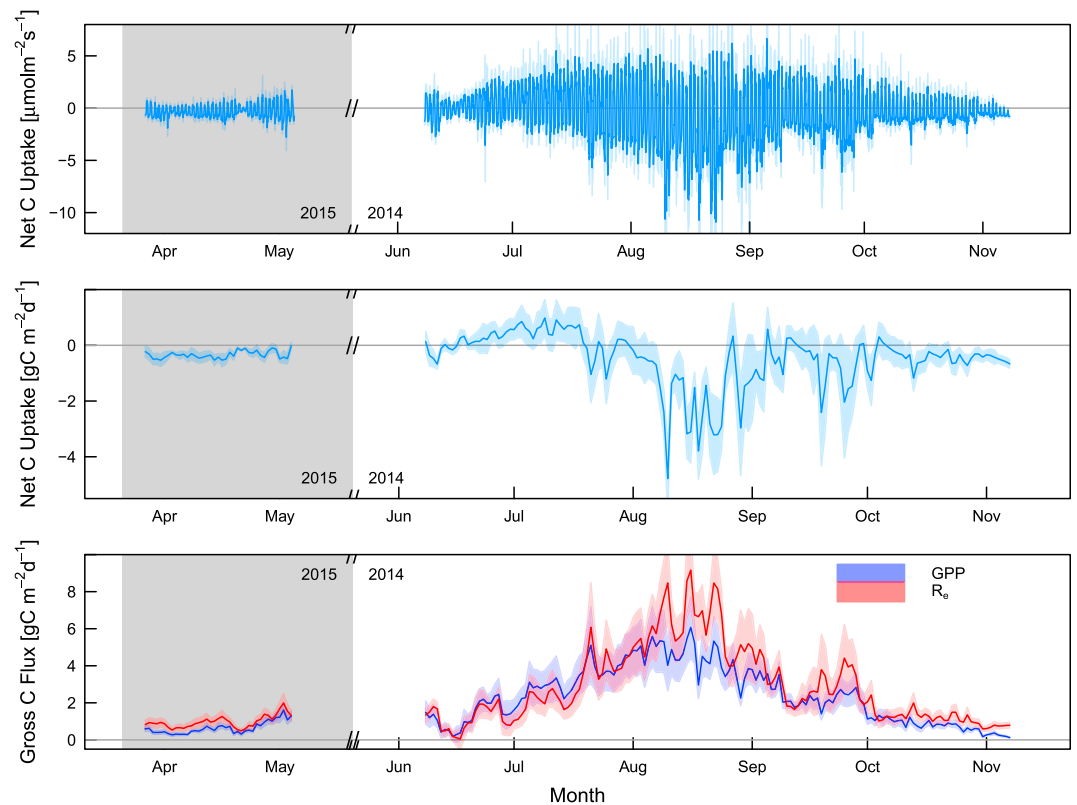


Figure 4. *Sphagnum*-peat CO₂ fluxes: (a) hourly NEE ($\mu\text{mol m}^{-2} \text{s}^{-1}$); (b) daily NEE ($\text{g C m}^{-2} \text{d}^{-1}$); and (c) R_e (red, $\text{g C m}^{-2} \text{d}^{-1}$) and GPP (blue, $\text{g C m}^{-2} \text{d}^{-1}$) based on partitioning of NEE. Mean of six chambers $\pm 95\%$ CIs. Positive NEE means net C uptake by the *Sphagnum*-peat system.

3.2. *Sphagnum*-Peat NEE, GPP, and R_e

Hourly measurements of net *Sphagnum*-peat CO₂ exchange (NEE; where positive values are uptake) show typical daily variation (Figure 4a). The amplitude in daily NEE increases steadily through the growing season to a maximum amplitude for 2 weeks in mid-August, the driest and warmest period, primarily driven by more negative nighttime values.

Daily integrated NEE shows peak C uptake midsummer (late June through mid-July) progressing to a strong net C loss to the atmosphere that corresponds to the maximum amplitude in the hourly data (Figure 4b). Indeed, for much of this composite growing season, the *Sphagnum*-peat system was a net C source to the atmosphere. The only sustained period of C uptake was from mid-June to mid-July, but we are cautious about making conclusions on an annual basis due to the composite nature of this data set and the missing data during May; we will return below to the implications of missing data for the annual C budget.

Both GPP and R_e showed very similar trajectories through the growing season (Figure 4c), as indicated by the hourly daytime and nighttime fluxes that were of similar magnitude during much of the growing season. In the early spring, both GPP and R_e were small. Interestingly, despite peak PAR and near peak temperature, GPP and R_e were also close to zero in mid-June and increased almost linearly (with of course high-frequency variation) to peak in early August (GPP) or mid-August (R_e). Over a similar timeframe, water table height declined steadily from a peak of around 45 mm to zero in early August and declined further to a summer minimum of -165 mm in mid-August. During August the GPP and R_e trajectories were less similar, and R_e continued to increase beyond the values of GPP leading to the large net C loss from the system during August. In other words, the substantial loss of C from the *Sphagnum*-peat system during mid-to-late summer was caused primarily by an increase in R_e (Figure 4c). This C loss was exacerbated by a subtle decline in GPP from early August.

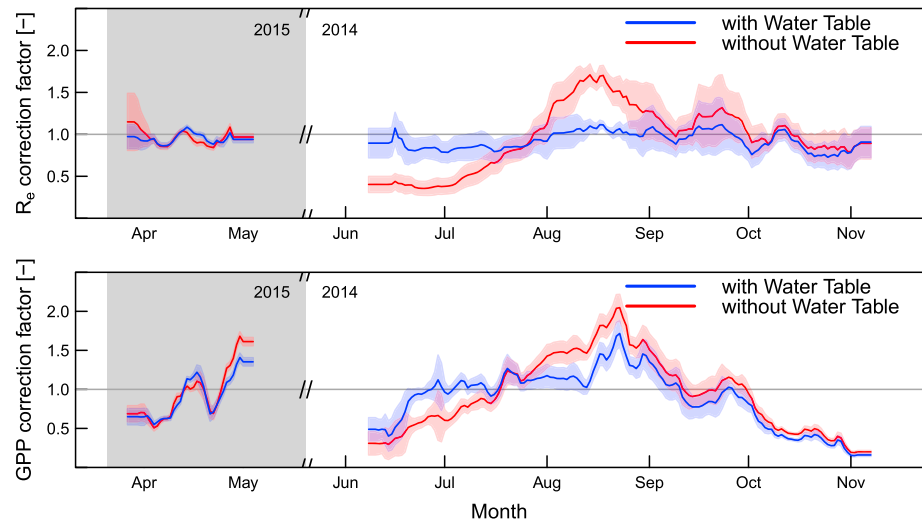


Figure 5. Trajectories of the *Barr et al.* [2004] empirical correction factor (mean \pm 95% CI) for (a) R_e ; and (b) GPP when water table is applied as a modifier of the basal R_e rate or maximum GPP (blue) or the flux partitioning functions are solely functions of temperature or PAR (red).

3.3. Effect of Water Table on Empirical Correction of Fluxes

To partition *Sphagnum*-peat NEE fluxes, we followed established methods [*Barr et al.*, 2004] previously applied to peatland systems [*Syed et al.*, 2006; *Sulman et al.*, 2012] but with the inclusion of water table as a modifier on the base rate of R_e (Eq (1)) or the maximum rate of GPP (equation (2)). To assess the impact of this nonstandard method including water table as a variable to partition fluxes, we investigate the dynamics of the empirical correction factor used to correct fluxes [*Barr et al.*, 2004] (Figure 5). For neither R_e nor GPP did the inclusion of water table affect the empirical correction factor in 2015 (April–May), because water table hardly varied during this period (Figure 3). However, in 2014 (June–November) water-level strongly affected the empirical correction factor for R_e such that there was no substantial variability in the correction factor over the period and for much of the time one was within the 95% CI of the correction factor (i.e., no correction). Not including water table as a modifier of the base R_e rate in the empirical Q_{10} function for R_e led to large overprediction of R_e by the flux partitioning during June and July, as indicated by a correction factor significantly below 1 (Figure 5a). The correction factor for R_e switched to above 1 during August, indicating underprediction of R_e during this period when only temperature was considered in the Q_{10} function.

Similarly for GPP, inclusion of water table as a modifier on the maximum rate of GPP resulted in an empirical correction factor that was closer to 1 than when GPP was assumed a function solely of PAR (Figure 5b). In contrast with R_e , there were still periods where the correction factor was substantially different from 1, even when water table was considered. Specifically, the correction factor was substantially below 1 during early June and in the late season (from late September). The correction factor was above one in mid-August suggesting that the empirical function of PAR and water table underestimated GPP during this period.

3.4. Effects of Biophysical Variables on Flux-Partitioned *Sphagnum* GPP

Wavelet analysis of the flux-partitioned GPP with temperature, PAR, precipitation, and water table height shows significant correlations to all these variables at different periods and at different times during the composite growing season (Figure 6). GPP correlations with temperature were in-phase and were strongest at biweekly to monthly periodicity in the early spring and late summer/fall (Figures 6a and 6b). Several times during the year, GPP showed correlations with temperature at lower daily to weekly frequencies, primarily in the same seasons but also in mid-July. GPP correlations to PAR were less clear and were more scattered through the time and frequency domain, though the correlations were often at similar frequencies and times as with temperature (Figures 6c and 6d). Notably, much of the high-frequency, early-spring (2015) GPP variability was correlated to temperature but not PAR. There is potential for autocorrelation in these measurements— R_e is calculated as a function of temperature and water table. A wavelet analysis of the more directly measured NEE also shows a similar correlation to temperature during 2015 (Figure S2).

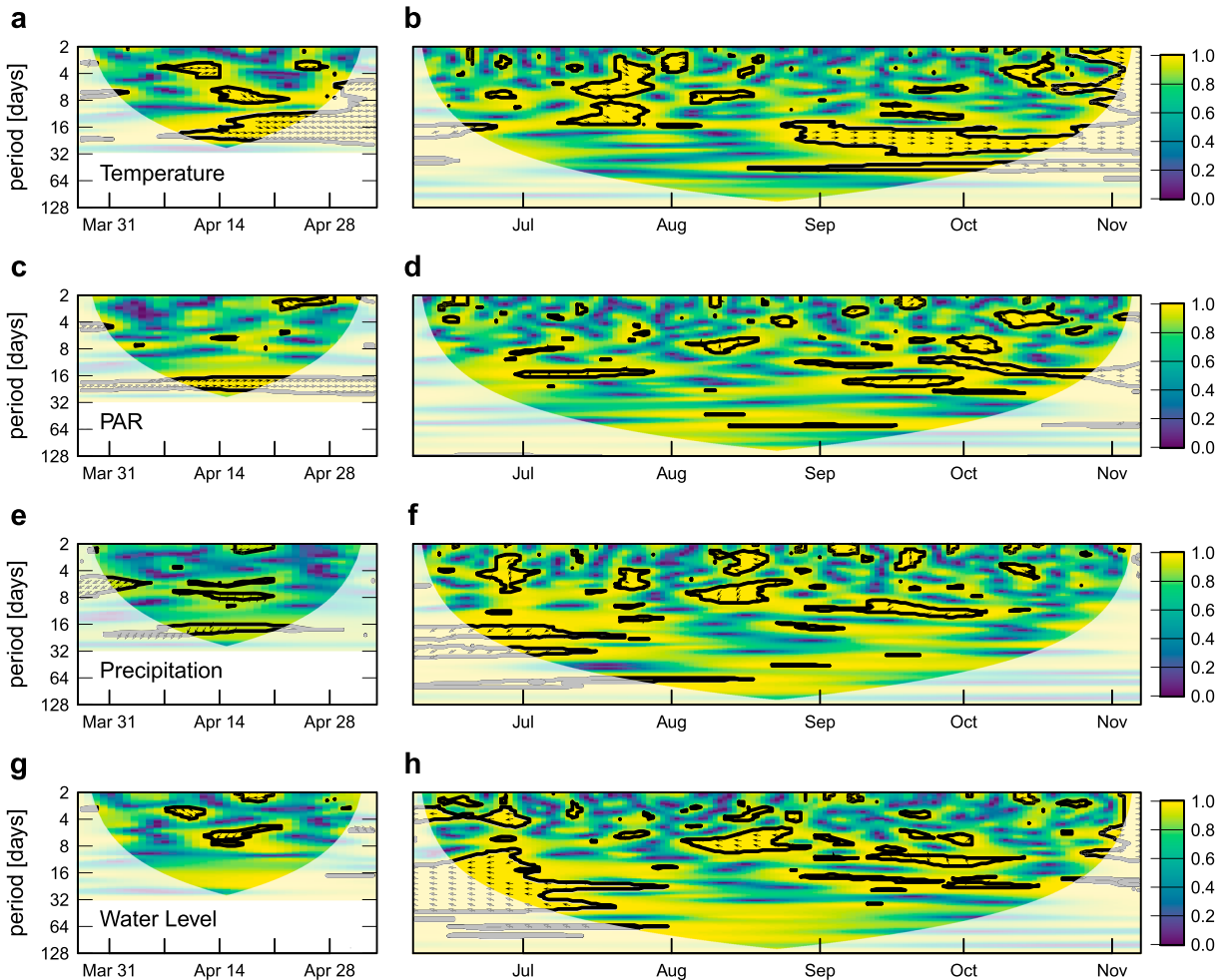


Figure 6. Wavelet coherence analysis of flux-partitioned GPP against meteorological and environmental variables. Values are equivalent to the coefficient of determination and describe the correlation between local wavelets of GPP and the environmental variable in question. Areas within black lines with arrows represent areas where the correlation is significant. Arrows represent phase differences of the wavelets; right pointing represents in-phase wavelets, left facing 180° out-of-phase, i.e., anti-phase; up or down represent 90° out-of-phase; bottom-left and top-right pointing indicate that GPP leads the environment variable, while bottom-right and top-left indicating the environment variable is leading GPP.

The GPP correlations with both precipitation and water table were often at similar frequencies and times, while correlations to water table were generally higher and covered larger patches within the time and frequency space (Figures 6e–6h). That correlation to precipitation and water table were similar is expected as precipitation is the primary driver of water table during most of the growing season (other than early in the season when the melt of seasonal snowpack and thawing of ice layers in peat dominate the water table, but this is a period that was not fully covered by our data set). The largest patch in the time and frequency domain where GPP was correlated with water table was in the early summer from early June stretching into mid-July and covering a range of low frequency variability from biweekly to bimonthly. Unfortunately, a substantial part of this correlation was on the edge of the time and frequency space, and a larger, more continuous data set would be desirable. The correlation with water table during this time was antiphase. There were also times of correlation at weekly periodicity during much of August and September. The periods and frequencies of correlations between GPP and temperature/PAR and water table/precipitation did not overlap (Figure 6). Again, there is potential for autocorrelation in these measurements— R_e is calculated as a function of temperature and water table. Nevertheless, a wavelet analysis of GPP when R_e was calculated using only a relationship to temperature shows a similar correlation with water table during the early summer of 2014 (Figure S3), suggesting that autocorrelation was minimal. The effect of autocorrelation would likely be a slight overestimation of the influence of temperature and water table and slight underestimation of the influence of PAR.

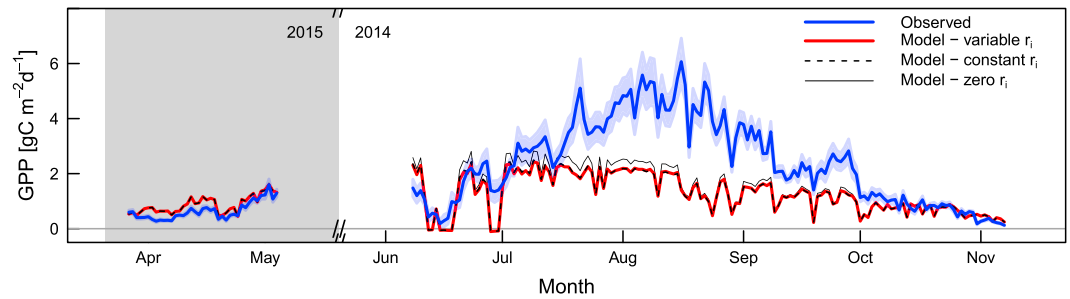


Figure 7. Modeled GPP (red and black lines) compared with flux-partitioned GPP (blue line and polygon). GPP was modeled with the *Williams and Flanagan* [1998] model with their representation of internal CO_2 resistance as a function of *Sphagnum* fresh weight dry weight ratio (red line), a constant internal CO_2 resistance (dotted black line), and zero internal CO_2 resistance (solid black line).

3.5. Effects of Biophysical Variables on Modeled *Sphagnum* GPP

Figure 7 shows the time series of flux-partitioned GPP and modeled GPP using the three r_i assumptions and parameterized after *Williams and Flanagan* [1998]. Some of the high-frequency variability (1–2 days—e.g., late August through September) and some medium-frequency variability (weekly—e.g., 2015 data) in GPP were captured by the model. The simulations with variable r_i produced GPP values that were almost identical to the simulations using the constant value of r_i , despite twofold variation in r_i (Figure S4), suggesting that temperature and PAR were more important drivers of daily and weekly GPP variability than *Sphagnum* water content.

Some weekly variability was not reproduced by the model (e.g., June through mid-July), nor was most variability in the low-frequency (monthly) domain. All three model simulations shown in Figure 7 were run with the assumption of boundary/water layer resistance (r_b) to CO_2 diffusion. There were few occasions during the season when the *Sphagnum* were submerged, providing sufficient illustration of the consequences of this assumption without masking the effect of other influential factors. The time periods when the *Sphagnum* were submerged are clear in the modeled GPP (mid and late June 2014) where GPP goes to zero. The orders of magnitude higher resistance to diffusion of CO_2 through water than air effectively prevents CO_2 diffusion almost as soon as *Sphagnum* becomes submerged. The model underpredicts GPP compared with the observations during these submerged time periods, though flux-partitioned GPP was clearly lower compared to other periods in June when the *Sphagnum* were not submerged (Figure 7). When the model was run with the assumption of zero r_b (i.e., no effect of submergence on CO_2 diffusion), GPP was strongly overpredicted during all periods when *Sphagnum* was submerged (Figure S5) suggesting that the observed drops in GPP during submerged periods could not be explained by PAR or temperature variability. Furthermore, the variable r_i was not able to account for the observed low values of flux-partitioned GPP when *Sphagnum* were submerged or close to submerged (June and early July 2014) suggesting that tissue water content was not a driver of these GPP lows.

During June and early July when the *Sphagnum* were not submerged, all three r_i assumptions overpredicted GPP. This overprediction was also apparent in all the April and May 2015 data and in the late season from mid-September in 2014. In contrast, all three r_i assumptions underpredicted GPP during the observed peak in flux-partitioned GPP—August and the first week of September. To further investigate these overpredictions and underpredictions, we ran the model with a number of different canopy scaling assumptions. The simulations in Figure 5 assume a shoot area index (SAI) of 2 and the canopy scaling parameters determined by *Williams and Flanagan* [1998]—a light extinction coefficient (k) of 1.5 and a canopy clumping coefficient (Ω) of 1 (i.e., no clumping). To investigate the effect of these assumptions, we investigated the consequences of varying these parameters: SAI at 1, 2, 3, and 4; k of 1 and 1.5; and Ω of 1 and 1.5 (Figure 8).

Varying these canopy scaling parameters has a strong influence on simulated GPP, with SAI variability having the most influence, partly because the range over which SAI was varied was larger than the range of k and Ω . In the early season and late season when the simulations in Figure 7 overpredicted GPP, assuming a SAI of 1 closely reproduced observations (Figure 8). The accurate predictions from SAI of 1 persisted in mid-June but could not reproduce the increase in GPP beginning toward the end of June.

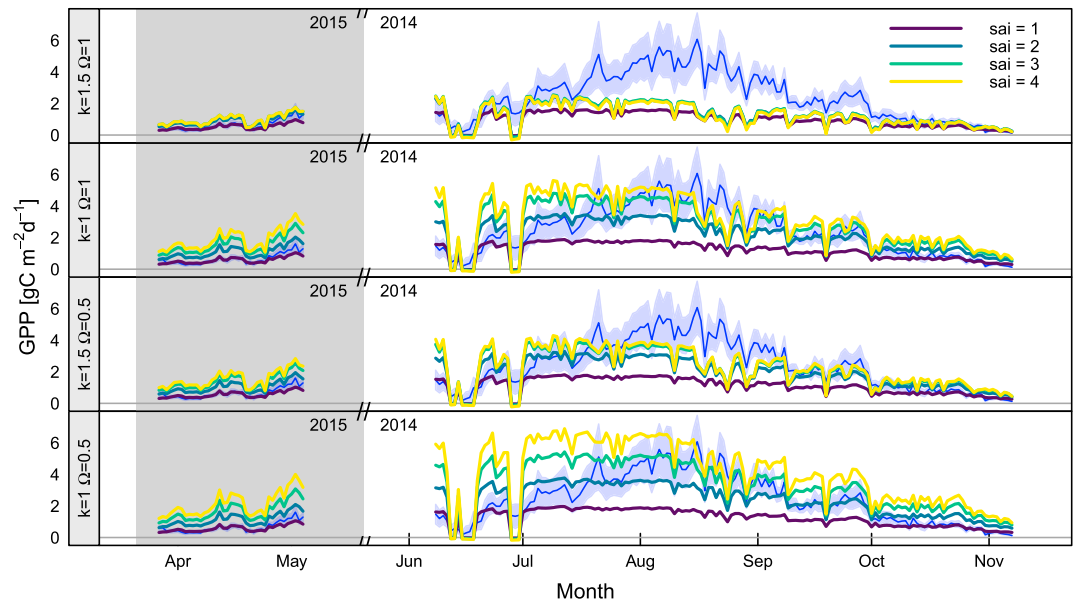


Figure 8. Modeled GPP when canopy scaling assumptions are varied compared with flux-partitioned GPP (blue line and polygon): (a) k of 1.5 and Ω of 1 as in Figure 6; (b) k of 1 and Ω of 1; (c) k of 1.5 and Ω of 0.5; and (d) k of 1 and Ω of 0.5. Colored lines (other than blue) represent different *Sphagnum* SAI: 1 (purple), 2 (gray blue), 3 (green), and 4 (yellow). GPP was modeled as above with the Williams and Flanagan [1998] model including their representation of internal CO_2 resistance as a function of *Sphagnum* fresh weight dry weight ratio.

Higher values of SAI (3 or 4 or both depending on values of k and Ω) were able to accurately reproduce the August peak in GPP, apart from with high k and high Ω (Figure 8a) in which the high extinction coefficient and no clumping prevented penetration of light to the lower stem layers. The assumptions best able to capture both the August peak in GPP, and the early September drop and lower GPP values thereon were with a k of 1.5 and Ω of 0.5, with a SAI of 3 and 4 which produced very similar results (Figure 8c). Despite this good prediction of low frequency variability in August and September, these assumptions were not able to reproduce the low-frequency variability from June to the end of July. Indeed, no combination of assumptions was able to accurately reproduce the GPP variability from June to the end of July.

The results of varying canopy scaling parameters suggest that no single set of assumptions can capture all the key features of the low-frequency variability in *Sphagnum* GPP for this composite season. In the early and late season, low amounts of actively photosynthesizing tissue (i.e., SAI of 1) reproduced flux-partitioned GPP most closely. Peak GPP during August and the drop through September was best reproduced by higher amounts of photosynthesizing tissue layers (SAI of 3 or 4) with k of 1.5 and Ω of 0.5. No assumption reproduced variability in the early summer, though simulating a water boundary layer caused by submergence of the *Sphagnum* suggested that some of the drops in flux-partitioned GPP during June could be related to submergence.

It is hypothesized that submergence is by degrees rather than a binary condition and that, within certain bounds, a receding water table progressively reveals more photosynthesizing tissue. It is also likely that the *Sphagnum* surface elevation is not fixed, with some potential to rise and fall with the water table. A logistic function of *Sphagnum* SAI to water table was hypothesized to represent this process. In combination with constant r_i , zero r_b , k of 1, and Ω of 0.5, including the logistic function for SAI resulted in good reproduction of the weekly variability in early summer of 2014 (Figure 9).

4. Discussion

Using a composite growing season of chamber flux measurements in an ombrotrophic *Sphagnum*-peat bog, we found that peak GPP was delayed relative to peak PAR. GPP increased to the peak during a time when water table was receding and showed the strongest variation. Wavelet analysis suggested that GPP and water table variation were significantly correlated during this period. Internal resistance to CO_2 diffusion as a

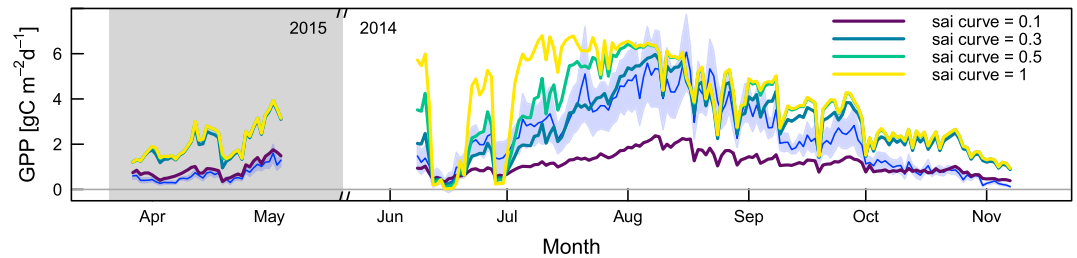


Figure 9. Modeled GPP including a hypothesis that SAI is a logistic function of water table height compared with flux-partitioned GPP (blue line and polygon); colored lines (other than blue) represent different curvature parameter, p_3 , values for the logistic curve: 0.1 (purple), 0.3 (gray blue), 0.5 (green), and 1.0 (yellow). GPP was modeled as above with p_1 (maximum SAI) of 3, k of 1, and Ω of 0.5 and without the *Williams and Flanagan* [1998] representation of internal CO_2 resistance.

function of *Sphagnum* water content [Williams and Flanagan, 1998] was our initial hypothesis for the control of *Sphagnum* GPP by water. However, when implemented in a mechanistic *Sphagnum* photosynthesis model [Farquhar et al., 1980; Williams and Flanagan, 1998; Weston et al., 2015] that responds to temperature and light, this hypothesis was not able to reproduce the increasing trend in GPP during this period (Figure 7). A simple, logistic function describing *Sphagnum* photosynthesizing tissue area in relation to water table was able to reproduce the dynamics of GPP during this period. Temperature and PAR also influenced daily and full season dynamics, but the model overpredicted GPP in the shoulder seasons. Wavelet analysis suggested these shoulder season dynamics were temperature related, and flux partitioning indicated a dynamic maximum rate of photosynthesis.

4.1. Seasonal Drivers of GPP: August–September

In line with previous field studies showing strong correlations of GPP and NEE [Glenn et al., 2006] with PAR in the field, summer through early autumn (August through September) GPP variability was related to variability in PAR. The relationship with PAR was demonstrated by the empirical flux-partitioning correction factor close to 1 during much of the period (Figure 5), the ability of some combinations of model assumptions to capture this variability (Figure 8b and c), and short periods of high-frequency correlations between wavelets (Figure 6 d). However, a late-August increase and peak in the correction factor suggests another biophysical variable that influenced GPP, and this mid-August GPP increase and peak was not captured by any model simulation. Also, the wavelet correlations with PAR were not substantial, and a role for water table height was indicated at weekly frequency during September (Figure 6h).

Simulations best able to reproduce the magnitude and the dynamics of GPP during the August–September summer period were those with relatively high SAI—3 and 4 (for k of 1.5 and Ω of 0.5) or 3 (for k of 1 and Ω of 1). It is likely that the *Sphagnum* at the site had either more photosynthesizing tissue or higher photosynthetic capacity per unit stem area during the late August increase in the empirical correction factor. Previous studies have indicated dynamic maximum photosynthetic capacity during the season both in field [Glenn et al., 2006; Syed et al., 2006; Adkinson and Humphreys, 2011; Adkinson et al., 2011; Flanagan and Syed, 2011] and laboratory measurements [Williams and Flanagan, 1998]. In the laboratory, Williams and Flanagan [1998] ascribed the variability to changes in physiological capacity per unit stem area and determined a light extinction coefficient (k) of 1.5 and SAI of 1.5 to achieve the correct curvature of the photosynthetic light response. A k of 1.5 precludes any influence on GPP of SAI above 2.5 (Figure 8) due to the strong attenuation of light through the canopy that high k causes.

The physical interpretation of a canopy extinction coefficient (k) is the projected leaf area on a two-dimensional plane perpendicular to the direct beam radiation. A value of 0.5 describes a random, also known as spherical, leaf-angle distribution while a value of 1 indicates a horizontal leaf area [Ross, 1981; Niinemets and Tobias, 2014]. While a value of 1.5 helps accurately describe the curvature observed in the response of *Sphagnum* C assimilation to PAR [Williams and Flanagan, 1998], it is difficult to interpret physically. A k above 1 suggests multiple layering of leaves (or in this case stem) within a “single” leaf layer and the analogy of a moss canopy, particularly *Sphagnum*, to a tree canopy begins to breakdown. *Sphagnum* leaves are one cell thick and are highly clustered on the stem, hence the use of SAI analogously to LAI in trees when modeling *Sphagnum* C assimilation [Williams and Flanagan, 1998]. Moss, and again in particular *Sphagnum*, canopies

are also highly clumped [Niinemets and Tobias, 2014]; a trait that was not investigated by Williams and Flanagan [1998]. The results presented here suggest that once clumping is accounted for, accurate characterization of maximum *Sphagnum* SAI in the field will be important.

4.2. Seasonal Drivers of GPP: April and October

The GPP in early spring and late autumn (April and October) was low ($<2 \text{ g C m}^{-2} \text{ d}^{-1}$) and was best predicted by simulations with a SAI of 1 (Figure 8), indicating low photosynthetic capacity. The low photosynthetic capacity during these periods was not related to water table height as indicated by the empirical correction factor below 1 during these periods (Figure 5) and the wavelet time series analysis (Figure 6). Wavelet analysis suggests that temperature influenced this low maximum photosynthetic capacity though not in a simple way—temperatures were lower in the spring than the autumn while the correction factor was lower (indicating stronger downregulation of maximum GPP) during the autumn. It is possible that below freezing temperatures may have triggered a physiological downregulation of photosynthetic capacity in the autumn as the hourly temperature record shows a sustained cold period where air temperature regularly dropped below 0°C . This cold period began close to the beginning of October, coinciding with the initiation of the autumn decline in the correction factor (Figure 5) and the point at which simulations with SAI of 1 coincided within the 95% CI of the flux-partitioned GPP. It is also possible that photoperiod may trigger the dynamics of photosynthetic traits. Characterizing the dynamics of *Sphagnum* photosynthetic traits during the growing season and assessment of their triggers will help model the seasonal dynamics of *Sphagnum* photosynthesis.

4.3. Seasonal Drivers of GPP: June–July

Wavelet analysis and the empirical correction factor of 1 during this period indicate a substantial role for water table height in *Sphagnum* photosynthesis. Water table height was used in the flux partitioning allowing potential circularity to enter this line of reasoning. When flux partitioning was conducted ignoring water table height, the results were not substantially affected (Figure S3), indicating that the importance of water table height is robust. Wavelet analysis also suggests that the influence of water table had waned by mid-July and that temperature variability was more closely related to GPP variability at weekly frequency during late July.

While simulating twofold variation in r_i , the hypothesis that r_i is a function of *Sphagnum* water content [Williams and Flanagan, 1998] had no detectable effect on GPP when compared against a constant r_i assumption (Figure 7). While our function of *Sphagnum* water content was empirical and not mechanistic, this result suggests that during this season variable r_i was not an important driver of GPP dynamics. Water table height has been shown to be an important driver of peatland NEE in the field [Weltzin et al., 2000; Bubier et al., 2003; Tuittila et al., 2004; Strack and Waddington, 2007; Yurova et al., 2007; Adkinson and Humphreys, 2011; Adkinson et al., 2011; Flanagan and Syed, 2011]. However, for most of these studies, water table height did not reach above 100 mm below the *Sphagnum* surface, reaching minima at 400 mm [Syed et al., 2006; Adkinson and Humphreys, 2011; Adkinson et al., 2011] and as much as 700 mm [Flanagan and Syed, 2011] below the surface, while the minimum observed water table in this study period was 280 mm below the *Sphagnum* surface during the measurement period. For example, long-term data from the S1 bog show that the water tables typically fluctuate within a 300 mm range during most years, though a maximum range of 1400 mm was measured during the year with lowest recorded precipitation [Sebestyen et al., 2011]. Even though not seen in our study, *Sphagnum* productivity is likely to be strongly impacted when the water table is too low for capillary rise of water. Beyond water table depths of 200–300 mm, capillarity can decrease as evidenced by reduced evapotranspiration from the *Sphagnum* surface [Boelter, 1964; Nichols and Brown, 1980]. It is likely that under drier regimes, with lower water tables and thus low *Sphagnum* water content, r_i would be a more important factor influencing GPP. The function of *Sphagnum* water content to water table height that we used was empirical and may not be accurate for this system. Ideally, for simulations in TEMs we suggest that for purposes of water movement, *Sphagnum* be simulated as the top soil layer to allow water movement to occur along pressure gradients and thus consistently simulate *Sphagnum* water content.

The hypothesis of binary submergence/nonsubmergence and boundary layer resistance to CO_2 diffusion, r_b , by the water layer predicted zero GPP during occasions when the *Sphagnum* was submerged by water, whereas the calculated GPP was positive albeit at a lower rate compared to adjoining time periods. Given the much lower CO_2 diffusivity of water compared with air, the assumption effectively yields a binary

submerged or not submerged character to r_b , where as soon as the *Sphagnum* becomes submerged, r_b transitions from zero to sufficiently high to completely inhibit photosynthesis. This is clearly visible in the simulations during June where GPP drops to zero (Figure 7). The simulations in which zero r_b was assumed (i.e., solely PAR and temperature driven) indicate that the drop in flux-partitioned GPP appears not to have been driven simply by light or temperature (Figure S5), suggesting a role for water limitation of r_b during these periods.

In reality, submergence is likely to be more gradual. The surface of the *Sphagnum* has some degree of roughness and is not a smooth two-dimensional plane. Also, the submergence of the *Sphagnum* is unlikely to be a binary condition; it is likely to be a gradual transition from one state to the other such that some of the photosynthesizing tissue may be submerged while other parts may be exposed to the atmosphere. Finally, the *Sphagnum* surface height is not static but is rather dynamic as *Sphagnum* are likely to float to some degree, grow above the water table during prolonged periods of near-surface saturation, and may collapse as the water table recedes.

The additional hypothesis that *Sphagnum* SAI is a logistic function of water table height captured the dynamics of *Sphagnum* GPP during this early summer period in 2014. Modeled GPP was sensitive to the SAI curve parameter (p_3), and in 2014 a p_3 of 0.3 gave a good fit to the data. In 2015, however, p_3 0.1 gave a better fit. In 2015 the water table was between 100 and 200 mm below the surface, and at that depth, there is no reason to assume that water table was restricting SAI. This was the period of spring thaw (Figures 2, 3, and S1b). The thaw may be interacting with *Sphagnum* SAI or seasonal dynamics in *Sphagnum* photosynthetic parameters, as discussed above. In our view the low value of the SAI curve (0.1) that creates the best fit of the model during this period is compensating for the lack of seasonal dynamics in *Sphagnum* photosynthetic parameters.

We recommend the adoption of a logistic function to represent the interaction of *Sphagnum* photosynthesizing tissue area with the water table when the water table is at the *Sphagnum* surface, as is often the case for hollow dwelling *Sphagnum* species. Accurate implementation of this hypothesis will require accurate measurements of the elevation of the *Sphagnum* surface relative to the water table. Also, the logistic function is highly sensitive to the choice of curvature parameter (Figure 9), and as an initial recommendation we suggest a value of 0.3. However, correct parameterization of the function requires an understanding of the roughness of the *Sphagnum* surface, the vertical area occupied by the *Sphagnum* photosynthesizing tissue and how SAI scales with vertical position, and the range within which the *Sphagnum* surface height is able to follow the water table height. Alternatively, data assimilation could be used for parameter estimation [Laloy and Vrugt, 2012] but with a knowledge of the aforementioned factors to constrain realistic ranges for the estimated parameters.

4.4. NEE and R_e

The purpose of this study was to investigate the drivers of seasonal variability in *Sphagnum* GPP—a key process required to accurately understand and model net C uptake of the *Sphagnum*-peat system. Here we briefly examine the NEE and R_e fluxes measured by the 8100 s in the context of other measurements at this site and in other peatland ecosystems. The *Sphagnum*-peat system in a hollow of the SI bog was a net C source to the atmosphere during the majority of this composite growing season. GPP and R_e both peaked during August, but peak R_e was greater than peak GPP (Figure 4c) thus the *Sphagnum*-peat system was a net C source to the atmosphere during August. The time of peak net C uptake was during the early summer, coinciding with a high water table.

At the SPRUCE study site, using a unique collar enclosure method (1.13 m²) that excluded trees (but likely not tree roots) Hanson et al. [2016] reported annual NEE ranging from a slight sink of -3.1 g C m⁻² yr⁻¹ in 2013 to a C source ranging from 21 to 65 g C m⁻² yr⁻¹ across 2011, 2012, and 2014 (our main year of measurement). Annual net CO₂ exchange for temperate bogs typically ranges from slight sources (10 g C m⁻² yr⁻¹) to slight sinks (-76 g C m⁻² yr⁻¹) depending on bog site and the variable environmental conditions including water table, snow cover, and day and nighttime temperatures [Lafleur et al., 2003; Sottocornola and Kiely, 2005; Hommeltenberg et al., 2014; Hurluck et al., 2016].

There have been numerous chamber studies and laboratory manipulations reporting strong links between R_e and water table [Bridgham and Richardson, 1992; Oechel et al., 1998; Strack and Waddington, 2007], yet this is

not always consistent [Bubier *et al.*, 1998; Dimitrov *et al.*, 2010]. Lafleur *et al.* [2005] argue that variability in the relationship of water table to R_e is the result of a complex interaction among peat quality (tissue decomposability) and oxygen availability for heterotrophic respiration. Determination of the factors controlling R_e in peatland ecosystems is an active and key area of research for the SPRUCE experiment and more broadly, but is beyond the scope of this study. The LI8100 measurements and flux partitioning gave maximum rates of R_e that were comparable to the measurements in Hanson *et al.* [2016] of close to $8 \mu\text{mol m}^{-2} \text{s}^{-1}$.

Also beyond the scope of this study but as a point of reference for the flux data, net primary production (NPP) of the *Sphagnum* community of the S1 bog was estimated from measurements of *Sphagnum* stem elongation, mass per unit stem length, C concentration, and number of stems per unit ground area. NPP during 2014 was 205 g C m^{-2} , approximately half of the GPP ($398 \text{ g C m}^{-2} \pm 55 \text{ s.e.m.}$) measured during the composite growing season (recognizing this is not a complete annual number but useful for comparison given GPP during the missing time period was likely to be small). This expected relationship between GPP and NPP generated from completely independent measurements increases our confidence in both estimates and will be the focus of further mechanistic studies.

In summary, to improve the representation of *Sphagnum* photosynthesis in TEMs, we identify four areas for further observation, experimentation, and model development: (1) characterization of seasonal photosynthetic trait variation and the triggers of this phenology; (2) characterization of a logistic SAI function of water table, including accurate measurement of *Sphagnum* surface height relative to the water table; (3) model *Sphagnum* as the “top” soil layer for water dynamics; and (4) characterization of *Sphagnum* “canopy” optical properties, extinction coefficient (k), clumping (Ω), and maximum SAI. *Sphagnum* are the key component of many peatland ecosystems, but they are not the only component and vascular plants, especially shrubs, have been shown to be favored by warming temperatures [Walker *et al.*, 2006; Bragazza *et al.*, 2013]. Understanding and modeling all of these complex dynamics will be necessary for accurate predictions of peatland ecosystem responses to global change. The warming and CO_2 enrichment at the SPRUCE experiment [Hanson *et al.*, 2017] will help to provide mechanistic understanding of the complex interactions in these at risk ecosystems.

Acknowledgments

We are especially grateful for the kind support from W. Robert Nettles III, Jana Phillips, and Carrie Dorrance. This material is based upon work supported by the U.S. Department of Energy, Office of Science, Office of Biological and Environmental Research, under contract DE-AC05-00OR22725. Contributions of SDS were supported by the Northern Research Station of the USDA Forest Service, which also supports the long-term research program at the Marcell Experimental Forest. All data presented in this manuscript can be found on the SPRUCE project data portal (<http://dx.doi.org/10.3334/CDIAC/spruce.039>).

References

- Adkinson, A. C., and E. R. Humphreys (2011), The response of carbon dioxide exchange to manipulations of *Sphagnum* water content in an ombrotrophic bog, *Ecohydrology*, 4(6), 733–743, doi:10.1002/eco.171.
- Adkinson, A. C., K. H. Syed, and L. B. Flanagan (2011), Contrasting responses of growing season ecosystem CO_2 exchange to variation in temperature and water table depth in two peatlands in northern Alberta, Canada, *J. Geophys. Res.*, 116, G01004, doi:10.1029/2010JG001512.
- Armentano, T. V., and E. S. Menges (1986), Patterns of change in the carbon balance of organic soil-wetlands of the temperate zone, *J. Ecol.*, 74(3), 755–774, doi:10.2307/2260396.
- Backeus, I. (1988), Weather variables as predictors of *Sphagnum* growth on a bog, *Holarctic Ecol.*, 11(2), 146–150.
- Barr, A. G., T. A. Black, E. H. Hogg, N. Kljun, K. Morgenstern, and Z. Nestic (2004), Inter-annual variability in the leaf area index of a boreal aspen-hazelnut forest in relation to net ecosystem production, *Agr. Forest Meteorol.*, 126(3–4), 237–255, doi:10.1016/j.agrformet.2004.06.011.
- Belyea, L. R., and N. Malmer (2004), Carbon sequestration in peatland: Patterns and mechanisms of response to climate change, *Global Change Biol.*, 10(7), 1043–1052, doi:10.1111/j.1529-8817.2003.00783.x.
- Bernacchi, C. J., C. Pimentel, and S. P. Long (2003), In vivo temperature response functions of parameters required to model RuBP-limited photosynthesis, *Plant, Cell Environ.*, 26(9), 1419–1430, doi:10.1046/j.0016-8025.2003.01050.x.
- Billings, W. D. (1987), Carbon balance of Alaskan tundra and taiga ecosystems: Past, present and future, *Quaternary Sci. Rev.*, 6(2), 165–177, doi:10.1016/0277-3791(87)90032-1.
- Boelter, D. H. (1964), Water storage characteristics of several peats in situ, *Soil Sci. Soc. Am. J.*, 28(3), 433–435, doi:10.2136/sssaj1964.03615995002800030039x.
- van Breemen, N. (1995), How *Sphagnum* bogs down other plants, *Trends Ecol. Evol.*, 10(7), 270–275, doi:10.1016/0169-5347(95)90007-1.
- Bragazza, L., J. Parisod, A. Buttler, and R. D. Bardgett (2013), Biogeochemical plant-soil microbe feedback in response to climate warming in peatlands, *Nat. Clim. Change*, 3(3), 273–277, doi:10.1038/nclimate1781.
- Bridgham, S. D., and C. J. Richardson (1992), Mechanisms controlling soil respiration (CO_2 and CH_4) in southern peatlands, *Soil Biol. Biochem.*, 24(11), 1089–1099, doi:10.1016/0038-0717(92)90058-6.
- Brooks, A., and G. D. Farquhar (1985), Effect of temperature on the CO_2/O_2 specificity of ribulose-1,5-bisphosphate carboxylase oxygenase and the rate of respiration in the light—Estimates from gas-exchange measurements on spinach, *Planta*, 165(3), 397–406.
- Bubier, J., P. Crill, A. Mosedale, S. Frolking, and E. Linder (2003), Peatland responses to varying interannual moisture conditions as measured by automatic CO_2 chambers, *Global Biogeochem. Cycles*, 17(2), 1066, doi:10.1029/2002GB001946.
- Bubier, J. L., P. M. Crill, T. R. Moore, K. Savage, and R. K. Varner (1998), Seasonal patterns and controls on net ecosystem CO_2 exchange in a boreal peatland complex, *Global Biogeochem. Cycles*, 12, 703–714, doi:10.1029/98GB02426.
- Cai, T., L. B. Flanagan, and K. H. Syed (2010), Warmer and drier conditions stimulate respiration more than photosynthesis in a boreal peatland ecosystem: Analysis of automatic chambers and eddy covariance measurements, *Plant Cell Environ.*, 33(3), 394–407, doi:10.1111/j.1365-3040.2009.02089.x.

- Ciais, P. et al. (2014), Carbon and other biogeochemical cycles, in *Climate Change 2013: The Physical Science Basis. Contribution of Working Group I to the Fifth Assessment Report of the Intergovernmental Panel on Climate Change*, pp. 465–570, Cambridge Univ. Press, Cambridge.
- Clymo, R. S. (1970), The growth of *Sphagnum*: Methods of measurement, *J. Ecol.*, *58*(1), 13–49, doi:10.2307/2258168.
- Clymo, R. S. (1984), The limits to peat bog growth, *Philos. Trans. R. Soc. Lond. B: Biol. Sci.*, *303*(1117), 605–654, doi:10.1098/rstb.1984.0002.
- D'Angelo, B., S. Gogo, F. Laggoun-Défarge, F. Le Moing, F. Jégou, and C. Guimbaud (2016), Soil temperature synchronisation improves representation of diel variability of ecosystem respiration in *Sphagnum* peatlands, *Agr. Forest Meteorol.*, *223*, 95–102, doi:10.1016/j.agrformet.2016.03.021.
- Dietze, M. C., et al. (2011), Characterizing the performance of ecosystem models across time scales: A spectral analysis of the North American Carbon Program site-level synthesis, *J. Geophys. Res.*, *116*, G04029, doi:10.1029/2011JG001661.
- Dimitrov, D. D., R. F. Grant, P. M. Lafleur, and E. R. Humphreys (2010), Modeling the effects of hydrology on ecosystem respiration at Mer Bleue bog, *J. Geophys. Res.*, *115*, G04043, doi:10.1029/2010JG001312.
- Dimitrov, D. D., R. F. Grant, P. M. Lafleur, and E. R. Humphreys (2011), Modeling the effects of hydrology on gross primary productivity and net ecosystem productivity at Mer Bleue bog, *J. Geophys. Res.*, *116*, G04010, doi:10.1029/2010JG001586.
- Dise, N., S. D. Sebestyen, E. S. Verry, and K. N. Brooks (2011), Carbon emissions from peatlands, in *Peatland Biogeochemistry and Watershed Hydrology at the Marcell Experimental Forest*, edited by R. K. Kolka et al., pp. 297–347, CRC Press, Boca Raton, Fla.
- Evans, J. R., R. Kaldenhoff, B. Genty, and I. Terashima (2009), Resistances along the CO₂ diffusion pathway inside leaves, *J. Exp. Bot.*, *60*(8), 2235–2248, doi:10.1093/jxb/erp117.
- Farquhar, G. D., S. von Caemmerer, and J. A. Berry (1980), A biochemical model of photosynthetic CO₂ assimilation in leaves of C₃ species, *Planta*, *149*(1), 78–90, doi:10.1007/BF00386231.
- Fisher, J. B., D. N. Huntzinger, C. R. Schwalm, and S. Sitch (2014), Modeling the terrestrial biosphere, *Annu. Rev. Environ. Resour.*, *39*(1), 91–123, doi:10.1146/annurev-environ-012913-093456.
- Flanagan, L. B., and K. H. Syed (2011), Stimulation of both photosynthesis and respiration in response to warmer and drier conditions in a boreal peatland ecosystem, *Global Change Biol.*, *17*(7), 2271–2287, doi:10.1111/j.1365-2486.2010.02378.x.
- Frolking, S., N. Roulet, and D. Lawrence (2009), Issues related to incorporating northern peatlands into global climate models, in *Carbon Cycling in Northern Peatlands*, edited by A. J. Baird et al., pp. 19–35, AGU, Washington, D. C.
- Frolking, S., N. T. Roulet, E. Tuittila, J. L. Bubier, A. Quillet, J. Talbot, and P. J. H. Richard (2010), A new model of Holocene peatland net primary production, decomposition, water balance, and peat accumulation, *Earth Syst. Dynam.*, *1*(1), 1–21, doi:10.5194/esd-1-1-2010.
- Glenn, A. J., L. B. Flanagan, K. H. Syed, and P. J. Carlson (2006), Comparison of net ecosystem CO₂ exchange in two peatlands in western Canada with contrasting dominant vegetation, *Sphagnum* and *Carex*, *Agr. Forest Meteorol.*, *140*(1–4), 115–135, doi:10.1016/j.agrformet.2006.03.020.
- Gorham, E. (1991), Northern peatlands: Role in the carbon cycle and probable responses to climatic warming, *Ecol. Appl.*, *1*(2), 182–195, doi:10.2307/1941811.
- Gorham, E., C. Lehman, A. Dyke, D. Clymo, and J. Janssens (2012), Long-term carbon sequestration in North American peatlands, *Quaternary Sci. Rev.*, *58*, 77–82, doi:10.1016/j.quascirev.2012.09.018.
- Griffiths, N. A., and S. D. Sebestyen (2016), Dynamic vertical profiles of peat porewater chemistry in a northern peatland, *Wetlands*, *1119–1130*, doi:10.1007/s13157-016-0829-5.
- Gunnarsson, U. (2005), Global patterns of *Sphagnum* productivity, *J. Bryolog.*, *27*(3), 269–279, doi:10.1179/174328205X70029.
- Hanson, D. T., S. Swanson, L. E. Graham, and T. D. Sharkey (1999), Evolutionary significance of isoprene emission from mosses, *Am. J. Bot.*, *86*(5), 634–639, doi:10.2307/2656571.
- Hanson, D. T., K. Renzaglia, and J. C. Villarreal (2014), Diffusion limitation and CO₂ concentrating mechanisms in Bryophytes, in *Photosynthesis in Bryophytes and Early Land Plants*, edited by D. T. Hanson and S. K. Rice, pp. 95–111, Springer, Netherlands.
- Hanson, P. J., J. S. Riggs, C. Dorrance, and L. A. Hook (2011), SPRUCE environmental monitoring data: 2010–2011, *Carbon Dioxide Information Analysis Center (CDIAC)*, doi:10.3334/CDIAC/spruce.001.
- Hanson, P. J., J. S. Riggs, W. R. Nettles, M. B. Krassovski, and L. A. Hook (2015), SPRUCE deep peat heating (DPH) environmental data, February 2014 through July 2015, *Carbon Dioxide Information Analysis Center (CDIAC)*, doi:10.3334/CDIAC/spruce.013.
- Hanson, P. J., A. L. Gill, X. Xu, J. R. Phillips, D. J. Weston, R. K. Kolka, J. S. Riggs, and L. A. Hook (2016), Intermediate-scale community-level flux of CO₂ and CH₄ in a Minnesota peatland: Putting the SPRUCE project in a global context, *Biogeochemistry*, *129*(3), 255–272, doi:10.1007/s10533-016-0230-8.
- Hanson, P. J., et al. (2017), Attaining whole-ecosystem warming using air and deep soil heating methods with an elevated CO₂ atmosphere, *Biogeosciences*, *14*, 861–883, doi:10.5194/bg-2016-449.
- Harley, P. C., J. D. Tenhunen, K. J. Murray, and J. Beyers (1989), Irradiance and temperature effects on photosynthesis of tussock tundra *Sphagnum* mosses from the foothills of the Philip Smith Mountains, Alaska, *Oecologia*, *79*(2), 251–259, doi:10.1007/BF00388485.
- Harley, P. C., R. B. Thomas, J. F. Reynolds, and B. R. Strain (1992), Modeling photosynthesis of cotton grown in elevated CO₂, *Plant Cell Environ.*, *15*(3), 271–282, doi:10.1111/j.1365-3040.1992.tb00974.x.
- Hommeltenberg, J., H. P. Schmid, M. Drösler, and P. Werle (2014), Can a bog drained for forestry be a stronger carbon sink than a natural bog forest? *Biogeosciences*, *11*(13), 3477–3493, doi:10.5194/bg-11-3477-2014.
- Humphreys, E. R., P. M. Lafleur, L. B. Flanagan, N. Hedstrom, K. H. Syed, A. J. Glenn, and R. Granger (2006), Summer carbon dioxide and water vapor fluxes across a range of northern peatlands, *J. Geophys. Res.*, *111*, G04011, doi:10.1029/2005JG000111.
- Hurkuck, M., C. Brümmer, and W. L. Kutsch (2016), Near-neutral carbon dioxide balance at a seminatural, temperate bog ecosystem, *J. Geophys. Res. Biogeosci.*, *121*, 370–384, doi:10.1002/2015JG003195.
- Kleinen, T., V. Brovkin, and R. J. Schuldt (2012), A dynamic model of wetland extent and peat accumulation: Results for the Holocene, *Biogeosciences*, *9*(1), 235–248, doi:10.5194/bg-9-235-2012.
- Kostka, J. E., D. J. Weston, J. B. Glass, E. A. Lilleskov, A. J. Shaw, and M. R. Turetsky (2016), The *Sphagnum* microbiome: New insights from an ancient plant lineage, *New Phytol.*, doi:10.1111/nph.13993.
- Krassovski, M. B., J. S. Riggs, L. A. Hook, W. R. Nettles, P. J. Hanson, and T. A. Boden (2015), A comprehensive data acquisition and management system for an ecosystem-scale peatland warming and elevated CO₂; Experiment, *Geosci. Instrum. Meth. Data Syst.*, *4*(2), 203–213, doi:10.5194/gi-4-203-2015.
- Lafleur, P. M., N. T. Roulet, J. L. Bubier, S. Frolking, and T. R. Moore (2003), Interannual variability in the peatland-atmosphere carbon dioxide exchange at an ombrotrophic bog, *Global Biogeochem. Cycles*, *17*(2), 1036, doi:10.1029/2002GB001983.
- Lafleur, P. M., T. R. Moore, N. T. Roulet, and S. Frolking (2005), Ecosystem respiration in a cool temperate bog depends on peat temperature but not water table, *Ecosystems*, *8*(6), 619–629, doi:10.1007/s10021-003-0131-2.

- Laloy, E., and J. A. Vrugt (2012), High-dimensional posterior exploration of hydrologic models using multiple-try DREAM(ZS) and high-performance computing, *Water Resour. Res.*, *48*, W01526, doi:10.1029/2011WR010608.
- Limpens, J., B. J. M. Robroek, M. M. P. D. Heijmans, and H. B. M. Tomassen (2008), Mixing ratio and species affect the use of substrate-derived CO₂ by *Sphagnum*, *J. Veg. Sci.*, *19*(6), 841–848, doi:10.3170/2008-8-18456.
- Loisel, J., A. V. Gallego-Sala, and Z. Yu (2012), Global-scale pattern of peatland *Sphagnum*; growth driven by photosynthetically active radiation and growing season length, *Biogeosciences*, *9*(7), 2737–2746, doi:10.5194/bg-9-2737-2012.
- Maseyk, K. S., T. G. A. Green, and D. Klinac (1999), Photosynthetic responses of New Zealand *Sphagnum* species, *New Zeal. J. Bot.*, *37*(1), 155–165, doi:10.1080/0028825X.1999.9512621.
- Medlyn, B. E., et al. (2002), Temperature response of parameters of a biochemically based model of photosynthesis. II. A review of experimental data, *Plant Cell Environ.*, *25*(9), 1167–1179, doi:10.1046/j.1365-3040.2002.00891.x.
- Monsi, M., and T. Saeki (1953), The light factor in plant communities and its significance for dry matter production, *Jpn. J. Bot.*, *14*, 22–52.
- Moore, T. R., N. T. Roulet, and J. M. Waddington (1998), Uncertainty in predicting the effect of climatic change on the carbon cycling of Canadian peatlands, *Clim. Change*, *40*(2), 229–245, doi:10.1023/A:1005408719297.
- Nichols, D. S., and J. M. Brown (1980), Evaporation from a *Sphagnum* moss surface, *J. Hydrol.*, *48*(3–4), 289–302, doi:10.1016/0022-1694(80)90121-3.
- Niinemets, Ü., and M. Tobias (2014), Scaling light harvesting from Moss “leaves” to canopies, in *Photosynthesis in Bryophytes and Early Land Plants*, edited by D. T. Hanson and S. K. Rice, pp. 151–171, Springer, Netherlands.
- Oechel, W. C., G. L. Vourlitis, S. J. Hastings, R. P. Ault, and P. Bryant (1998), The effects of water table manipulation and elevated temperature on the net CO₂ flux of wet sedge tundra ecosystems, *Global Change Biol.*, *4*(1), 77–90, doi:10.1046/j.1365-2486.1998.00110.x.
- Olson, D. M., T. J. Griffis, A. Noormets, R. Kolka, and J. Chen (2013), Interannual, seasonal, and retrospective analysis of the methane and carbon dioxide budgets of a temperate peatland, *J. Geophys. Res. Biogeosci.*, *118*, 226–238, doi:10.1002/jgrg.20031.
- Parsekian, A. D., L. Slater, D. Ntargiannis, J. Nolan, S. D. Sebestyey, R. K. Kolka, and P. J. Hanson (2012), Uncertainty in peat volume and soil carbon estimated using ground-penetrating radar and probing, *Soil Sci. Soc. Am. J.*, *76*(5), 1911, doi:10.2136/sssaj2012.0040.
- Pitman, A. J. (2003), The evolution of, and revolution in, land surface schemes designed for climate models, *Int. J. Climatol.*, *23*(5), 479–510.
- R Core Development Team (2016), R: A language and environment for statistical computing, R Foundation for Statistical Computing, Vienna.
- Reichstein, M., et al. (2005), On the separation of net ecosystem exchange into assimilation and ecosystem respiration: Review and improved algorithm, *Global Change Biol.*, *11*(9), 1424–1439, doi:10.1111/j.1365-2486.2005.001002.x.
- Roesch, A., and H. Schmidbauer (2014), WaveletComp: Computational wavelet analysis.
- Ross, J. (1981) *The Radiation Regime and Architecture of Plant Stands*, Springer, Dordrecht, Netherlands.
- Roulet, N. T., P. M. Lafleur, P. J. H. Richard, T. R. Moore, E. R. Humphreys, and J. Bubier (2007), Contemporary carbon balance and late Holocene carbon accumulation in a northern peatland, *Global Change Biol.*, *13*(2), 397–411, doi:10.1111/j.1365-2486.2006.01292.x.
- Rydin, H., J. K. Jeglum, and K. D. Bennett (2013), *The Biology of Peatlands*, the Biology of Habitats Series, 2nd edn., Oxford Univ. Press, Oxford.
- Schipperges, B., and H. Rydin (1998), Response of photosynthesis of *Sphagnum* species from contrasting microhabitats to tissue water content and repeated desiccation, *New Phytol.*, *140*(4), 677–684, doi:10.1046/j.1469-8137.1998.00311.x.
- Sebestyey, S. D., C. Dorrance, D. M. Olson, E. S. Verry, R. K. Kolka, A. E. Elling, and R. Kyllander (2011), Long-term monitoring sites and trends at the Marcell experimental Forest, in *Peatland Biogeochemistry and Watershed Hydrology at the Marcell Experimental Forest*, edited by R. K. Kolka et al., pp. 15–71, CRC Press, Boca Raton, Fla.
- Sellers, P. J., J. A. Berry, G. J. Collatz, C. B. Field, and F. G. Hall (1992), Canopy reflectance, photosynthesis, and transpiration .3. A reanalysis using improved leaf models and a new canopy integration scheme, *Remote Sens. Environ.*, *42*(3), 187–216.
- Shi, X., P. E. Thornton, D. M. Ricciuto, P. J. Hanson, J. Mao, S. D. Sebestyey, N. A. Griffiths, and G. Bisht (2015), Representing northern peatland microtopography and hydrology within the community land model, *Biogeosciences*, *12*(21), 6463–6477, doi:10.5194/bg-12-6463-2015.
- Smith, E. L. (1937), The influence of light and carbon dioxide on photosynthesis, *J. Gen. Physiol.*, *20*(6), 807–830, doi:10.1085/jgp.20.6.807.
- Sottocornola, M., and G. Kiely (2005), An Atlantic blanket bog is a modest CO₂ sink, *Geophys. Res. Lett.*, *32*, L23804, doi:10.1029/2005GL024731.
- St-Hilaire, F., J. Wu, N. T. Roulet, S. Frolking, P. M. Lafleur, E. R. Humphreys, and V. Arora (2010), McGill wetland model: Evaluation of a peatland carbon simulator developed for global assessments, *Biogeosciences*, *7*(11), 3517–3530, doi:10.5194/bg-7-3517-2010.
- Stoy, P. C., et al. (2009), Biosphere-atmosphere exchange of CO₂ in relation to climate: A cross-biome analysis across multiple time scales, *Biogeosciences*, *6*(10), 2297–2312, doi:10.5194/bg-6-2297-2009.
- Strack, M., and J. M. Waddington (2007), Response of peatland carbon dioxide and methane fluxes to a water table drawdown experiment, *Global Biogeochem. Cycles*, *21*, GB1007, doi:10.1029/2006GB002715.
- Strack, M., J. M. Waddington, R. A. Bourbonniere, E. L. Buckton, K. Shaw, P. Whittington, and J. S. Price (2008), Effect of water table drawdown on peatland dissolved organic carbon export and dynamics, *Hydrol. Process.*, *22*(17), 3373–3385, doi:10.1002/hyp.6931.
- Sulman, B. N. et al. (2012), Impact of hydrological variations on modeling of peatland CO₂ fluxes: Results from the North American Carbon Program site synthesis, *J. Geophys. Res.*, *117*, G01031, doi:10.1029/2011JG001862.
- Syed, K. H., L. B. Flanagan, P. J. Carlson, A. J. Glenn, and K. E. Van Gaalen (2006), Environmental control of net ecosystem CO₂ exchange in a treed, moderately rich fen in northern Alberta, *Agr. Forest Meteorol.*, *140*(1–4), 97–114, doi:10.1016/j.agrformet.2006.03.022.
- Tuittila, E.-S., H. Vasander, and J. Laine (2004), Sensitivity of C sequestration in reintroduced *Sphagnum* to water-level variation in a cutaway peatland, *Restoration Ecol.*, *12*(4), 483–493, doi:10.1111/j.1061-2971.2004.00280.x.
- Turetsky, M., K. Wieder, L. Halsey, and D. Vitt (2002), Current disturbance and the diminishing peatland carbon sink, *Geophys. Res. Lett.*, *29*(11), 1526, doi:10.1029/2001GL014000.
- Walker, M. D., et al. (2006), Plant community responses to experimental warming across the tundra biome, *Proc. Natl. Acad. Sci.*, *103*(5), 1342–1346, doi:10.1073/pnas.0503198103.
- Wang, Y. P. (2003), A comparison of three different canopy radiation models commonly used in plant modelling, *Funct. Plant Biol.*, *30*(2), 143, doi:10.1071/FP02117.
- Wania, R., I. Ross, and I. C. Prentice (2009), Integrating peatlands and permafrost into a dynamic global vegetation model: 2. Evaluation and sensitivity of vegetation and carbon cycle processes, *Global Biogeochem. Cycles*, *23*, GB3015, doi:10.1029/2008GB003413.
- Weltzin, J. F., J. Pastor, C. Harth, S. D. Bridgman, K. Updegraff, and C. T. Chapin (2000), Response of bog and fen plant communities to warming and water-table manipulations, *Ecology*, *81*(12), 3464–3478, doi:10.1890/0012-9658(2000)081[3464:ROBAFP]2.0.CO;2.
- Weston, D. J., C. M. Timm, A. P. Walker, L. Gu, W. Muchero, J. Schmutz, A. J. Shaw, G. A. Tuskan, J. M. Warren, and S. D. Wullschlegel (2015), *Sphagnum* physiology in the context of changing climate: Emergent influences of genomics, modelling and host–microbiome interactions on understanding ecosystem function, *Plant Cell Environ.*, *38*(9), 1737–1751, doi:10.1111/pce.12458.
- Wieder, R. K., K. D. Scott, K. Kamminga, M. A. Vile, D. H. Vitt, T. Bone, B. Xu, B. W. Benschoter, and J. S. Bhatti (2009), Postfire carbon balance in boreal bogs of Alberta, Canada, *Global Change Biol.*, *15*(1), 63–81, doi:10.1111/j.1365-2486.2008.01756.x.

- Williams, T. G., and L. B. Flanagan (1996), Effect of changes in water content on photosynthesis, transpiration and discrimination against $^{13}\text{CO}_2$ and $\text{C}^{18}\text{O}^{16}\text{O}$ in *Pleurozium* and *Sphagnum*, *Oecologia*, *108*(1), 38–46, doi:10.1007/BF00333212.
- Williams, T. G., and L. B. Flanagan (1998), Measuring and modelling environmental influences on photosynthetic gas exchange in *Sphagnum* and *Pleurozium*, *Plant, Cell Environ.*, *21*(6), 555–564, doi:10.1046/j.1365-3040.1998.00292.x.
- Wu, J., and N. T. Roulet (2014), Climate change reduces the capacity of northern peatlands to absorb the atmospheric carbon dioxide: The different responses of bogs and fens, *Global Biogeochem. Cycles*, *28*, 1005–1024, doi:10.1002/2014GB004845.
- Yu, Z., J. Loisel, D. P. Brosseau, D. W. Beilman, and S. J. Hunt (2010), Global peatland dynamics since the last glacial maximum, *Geophys. Res. Lett.*, *37*, L13402, doi:10.1029/2010GL043584.
- Yurova, A., A. Wolf, J. Sagerfors, and M. Nilsson (2007), Variations in net ecosystem exchange of carbon dioxide in a boreal mire: Modeling mechanisms linked to water table position, *J. Geophys. Res.*, *112*, G02025, doi:10.1029/2006JG000342.